Since January 2020 Elsevier has created a COVID-19 resource centre with free information in English and Mandarin on the novel coronavirus COVID-19. The COVID-19 resource centre is hosted on Elsevier Connect, the company's public news and information website.

Virology 454-455 (2014) 270–279

Contents lists available at ScienceDirect

Virology

journal homepage: www.elsevier.com/locate/yviro

Rotavirus infection induces G1 to S phase transition in MA104 cells via Ca^{+2}/Calmodulin pathway

Rahul Bhowmick, George Banik, Shampa Chanda, Shiladitya Chattopadhyay, Mamta Chawla-Sarkar*

Division of Virology, National Institute of Cholera and Enteric Diseases, P-33, C.I.T. Road Scheme-XM, Beliaghata, Kolkata 700010, West Bengal, India

ARTICLE INFO

Article history:
Received 23 December 2013
Returned to author for revisions
20 January 2014
Accepted 2 March 2014
Available online 21 March 2014

Keywords:
Rotavirus
Cell cycle
Calmodulin

ABSTRACT

Viruses, obligate cellular parasites rely on host cellular functions and target the host cell cycle for their own benefit. In this study, effect of rotavirus infection on cell cycle machinery was explored. We found that rotavirus (RV) infection in MA104 cells induces the expression of cyclins and cyclin dependent kinases and down-regulates expression of CDK inhibitors, resulting in G1 to S phase transition. The rotavirus induced S phase accumulation was found to be concurrent with induction in expression of calmodulin and activation of CaMKI which is reported as inducer of G1–S phase transition. This cell cycle manipulation was found to be Ca^{+2}/Calmodulin pathway dependent. The physiological relevance of G1 to S phase transition was established when viral gene expressions as well as viral titers were found to be increased in S phase synchronized cells and decreased in G0/G1 phase synchronized cells compared to unsynchronized cells during rotavirus infection.

Introduction

Manipulating the cell cycle machinery in order to sustain their own replication is a common mechanism employed by different viruses (Emmett et al., 2005). Among the three check points of cell cycle at G_1/S, G_2/M and the metaphase/anaphase boundary, G_1/S is the time window where cell decides for growth or quiescence depending on environmental conditions (Bartek and Lukas, 2001). During the hours preceding the G_1 phase, Retinoblastoma (Rb) remains in hypo phosphorylated form, which can bind and inhibit a group of transcription factors (like E2F) responsible for transcribing genes required for replication as well as cell cycle progression (Giacinti and Giordano, 2006). When cell gets stimuli essential for the G_1 to S phase transition, Rb becomes hyperphosphorylated and loses ability to bind and inhibit E2F, which then translocates to nucleus and induces expression of genes like thymidine kinase, thymidine synthetase, dihydrofolate reductase, cyclins and CDKs required for G1 to S phase transition (Harbour and Dean, 2000; Fan and Bertino, 1997). Ca^{+2}/CaM-stimulated proteins, including the family of multifunctional Ca^{+2}/CaM-stimulated protein kinases (CaMK), have been identified as one of the important mediators among several stimuli that induce cell cycle progression (Kahl and Means, 2003). CaMKI induces Rb phosphorylation and cyclin D1 upregulation and CDK 4 activation for overall G1 to S phase transition (Skelding et al., 2011).

Viruses are obligate parasites which lack many of the proteins required for genome replication, so they rely on the host cell for resources and target their cell cycle check points to create a favorable environment for their own replication (Schang, 2003). DNA viruses are extensively studied for cell cycle manipulation as primary site of their replication is in the nucleus. To support viral replication small DNA viruses lacking their own polymerase, such as simian virus 40 (DeCaprio et al., 1988; Fanning and Knippers, 1992), human papillomavirus (Werness et al., 1990) and adenovirus (Eckner et al., 1994; Howe et al., 1990) promote cell cycle progression to S phase. To avoid competition with host for replication machinery large DNA viruses (herpes viruses) arrest cell cycle in the G_0/G_1 phase (Flemington, 2001). Retroviruses such as HIV type 1 arrests cell cycle in G_2/M phase by employing Vpr protein for proper viral gene expression (Goh et al., 1998; He et al., 1995). Single stranded RNA viruses, whose primary site of replication is cytoplasm were also been found to affect host cell cycle either inducing G_2/M phase arrest (infectious bronchitis virus) (Dove et al., 2006) or G_0/G_1 arrest (murine corona virus, Influenza virus) (Chen and Makino, 2004; He et al., 2010), however whether self-limiting double stranded RNA viruses like RV manipulates cell cycle remains largely unknown.

RV, a nonenveloped double stranded RNA virus of reoviridae family is an important threat to mankind as it causes over 5 million deaths each year with >85% of these deaths occurring in children aged below five years in developing countries (Rossen et al., 2004; Estes and Kapikian, 2007). In addition it also infects live stocks, thus

* Corresponding author. Tel.: +91 33 2353 7470; fax: +91 33 2370 5066.
E-mail addresses: chawlam70@gmail.com, sarkarmc@icmr.org.in (M. Chawla-Sarkar).

http://dx.doi.org/10.1016/j.virol.2014.03.001
0042-6822

it has huge economic importance. The virus with its 11 segmented ds RNA genome encodes six structural proteins (VP1 to VP4, VP6 and VP7) which form the structure of the virus particle and six non-structural proteins (NSP1 to NSP6), which like non-structural proteins of other viruses confirm viral replication and establish infection in host cells (Autret et al., 2008; Bitko et al., 2007; Bollati et al., 2009; Ehrhardt et al., 2007; Foy et al., 2003; Holloway et al., 2009; Spann et al., 2004; Talon et al., 2000).

Previous studies have identified mechanisms by which RV activates PI3K/AKT pathway (Bagchi et al., 2010) or degrades p53 (Bhowmick et al., 2013) to subvert host innate immune system that tries to induce programmed cell death in response to viral infection (Roulston et al., 1999). Many observations such as sharing of same morphological characters (Cell shrinkage, chromatin condensation and membrane blebbing) and regulatory proteins (p53, Rb, E2F) suggests link between apoptosis and cell cycle regulation, which prompted us to explore the effect of RV infection on cell cycle (Alenzi, 2004).

In this study we attempted to understand effect of RV infection on host cell cycle machinery and its implication on virus infectivity. We found that RV induces higher proportion of cells to accumulate in S phase during infection by activating Ca^{+2}/CaM pathway. Accumulation of cells in S phase during initial stage of infection may benefit RV in executing proper life cycle.

Results

RV infection induces cells to accumulate in S phase in a strain independent manner

Based on the observation that RV inhibits apoptosis and induces survival pathways during early infection (Bagchi et al., 2010; Bhowmick et al., 2012), we examined whether RV can also regulate cell cycle especially during early infection by infecting MA104 cells with SA11 (G3P2), A5-13 (G8P1) and OSU (G5P7) strains of RV at 3 moi (multiplicity of infection) or keeping them mock infected for increasing time points. Cells were then treated with propidium iodide (50 μg/ml) and cell cycle status was analyzed using flowcytometry as described in material and methods. As shown in Fig. 1A significant accumulation (20–32%) of infected cells in S phase was observed during early time point of infection (2–6 hpi), compared to mock infected cells (10–11%) in a strain independent manner. Whereas at 8 hpi number of cells in S phase was not significantly higher (14–16%) in case of all the three strains, compared to uninfected controls (10–11%) and at later time points (10–12 hpi) no of cells started to increase in sub G_0 phase compared to uninfected control (Fig. 1A). To confirm the direct effect of RV on host cell cycle machinery, MA104 cells were synchronized in G_1 phase by serum starvation and were infected with SA11 at 3 moi or kept mock infected followed by cell cycle analysis using flowcytometry. Cell cycle analysis revealed an increased accumulation of cells (20–30%) in S phase in SA11 infected cells compared to mock infected cells (9–10%) (Fig. 1B). To know whether this cell cycle modulation is viral replication dependent or not, SA11 was inactivated with UV irradiation (Li et al., 2009) and MA104 cells were infected with UV inactivated virus or live virus. Cells were collected at indicated time points and subjected to flowcytometry analysis. It was found that viral replication is necessary for cell cycle manipulation as no significant accumulation of infected cells in S phase was observed in UV inactivated virus infected cells whereas active live virus induced S phase accumulation (Fig. 1A). Thus overall results suggest RV manipulates cell cycle machinery to drive cells from G_1 to S phase.

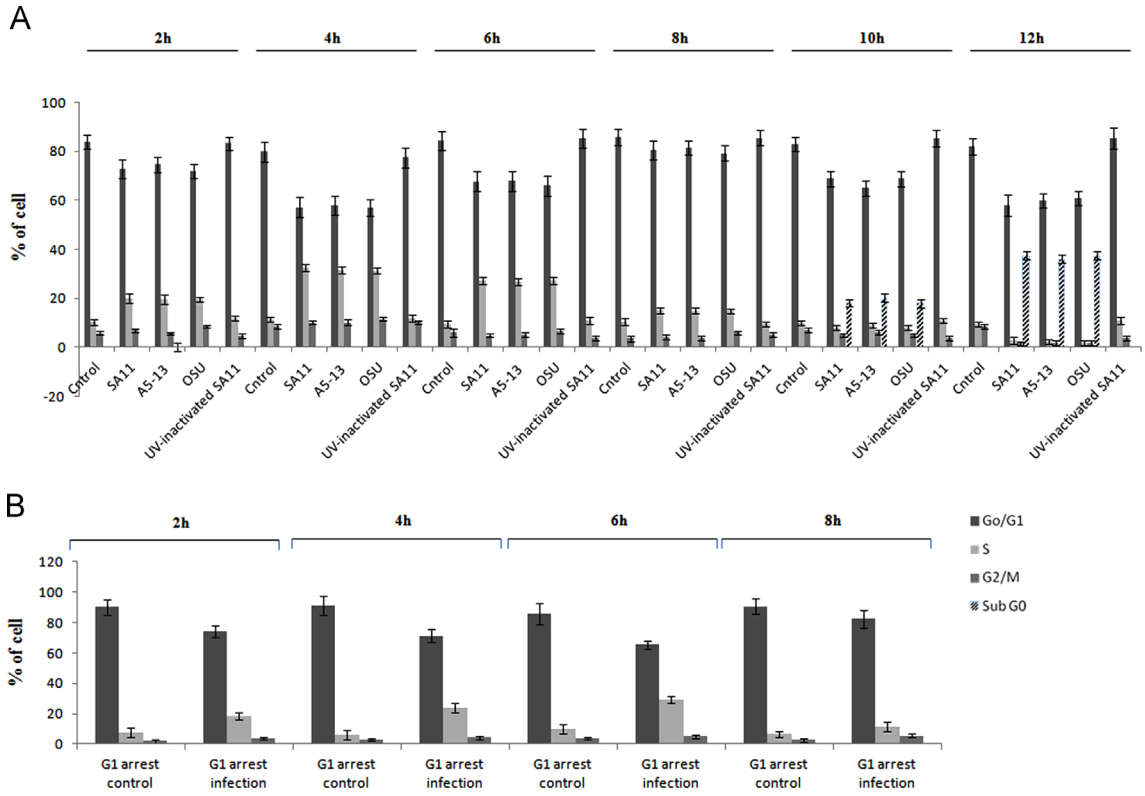

Fig. 1. RV induces G_1 to S phase transition in a strain independent but viral replication dependent manner. (A) MA104 cells were infected with SA11 or A513 or OSU or UV inactivated SA11 strain for 2–12 h or kept mock infected followed by propidium iodide (50 μg/ml) staining and cell cycle analysis using BD FACSAria II flow cytometer. Each bar represent % of cell present in specific phase of cell cycle. Results are representative (mean ± SD) of three independent experiments. (B) MA104 cells were serum starved for 48 h followed by SA11 infection at 3 moi for indicated time points or kept mock infected followed by cell cycle analysis. Each bar represents % of cell present in specific phase of cell cycle. Results are representative (mean ± SD) of three independent experiments.

RV infection induces activation of E2F by phosphorylating Rb

The retinoblastoma (Rb) protein is the central molecule which controls the G_1/S transition by connecting all the signals important for the decision of transition with transcription machinery (Weinberg, 1995). To know the phosphorylation status of Rb during RV infection, MA104 cells were infected with the RV SA11 strain (at a moi of 3) and incubated for 0–8 hpi. Cell extracts were immunoblotted with phospho Rb specific antibody. Compared to mock infected cells RV infection induced Rb hyper phosphorylation during early infection (2–6 hpi) but from 8 hpi onwards the Rb phosphorylation was reduced (Fig. 2A lower panel). Furthermore, to monitor the downstream effect of Rb phosphorylation, nuclear fractions of same set of experiments was immunoblotted with E2F specific antibody to analyze level of activated E2F. Results revealed increased translocation of E2F into nucleus during early infection (2–6 hpi), which is concurrent with Rb hyper phosphorylation (Fig. 2A upper panel) confirming the G1 to S phase stimulation during the early hours of RV infection. In addition to nuclear translocation, expression of E2F gene was also induced during RV infection as assessed by immunoblotting and real time PCR (Fig. 2B). Functionality of increased nuclear translocation of E2F was further validated by assessing expression of different E2F regulated genes such as thymidine kinase, thymidine synthase and dihydrofolate reductase in SA11 infected MA104 cells by quantitative RT-PCR. As shown in Fig. 2C, all three E2F regulated genes were significantly upregulated during 2–4 hpi consistent with nuclear translocation of E2F.

RV infection activates G_1 cyclin dependent kinases by modulating expression levels of cyclin, CDKs and CDKIs

Since Rb hyper phosphorylation was observed during RV infection, the expression levels of Cyclin and CDK's following SA11 (3 moi) infection were assessed by either immunoblotting or quantitative RT-PCR. Compared to mock infected cells expression of both transcript and protein levels of Cyclin D1, cyclin D3 and CDK4, CDK6 was induced in SA11 infected cells during 2–6 hpi followed by decrease at 8 hpi. Cyclin E1 and CDK2 transcripts were induced as early as 2 hpi but significant increase in protein level were observed at 4–6 hpi (Fig. 3A and B). As expression of both CDK and Cyclin increased during infection, kinase activity of CDK4, CDK6 and CDK2 was evaluated by immunoprecipitating cyclin-CDK complexes from SA11 (3 moi) infected and mock infected cells. The kinase activity of cyclin-CDK complex was measured by incubating (30 min at 37 °C) them with specific substrates such as Rb for CDK4, CDK6 and Histone H1 for CDK2 *in vitro* in specific kinase buffer followed by immunoblotting with pRb and pHistone H1 specific antibody. Increases in activity were observed for CDK4, CDK6 during early infection (2–6 hpi) whereas CDK2 was transiently activated only at 4–6 hpi (Fig. 3C). Activation of CDKs depends on the level of CDK inhibitors. To assess whether RV modulates expression of CDK inhibitors to regulate cell cycle, whole cell lysates or total RNA of MA104 cells infected with either SA11 (3 moi) or mock infected were subjected to either immunoblotting or real time PCR with p15, p21, p27 specific antibodies or primers, respectively. Results revealed that representative CDK

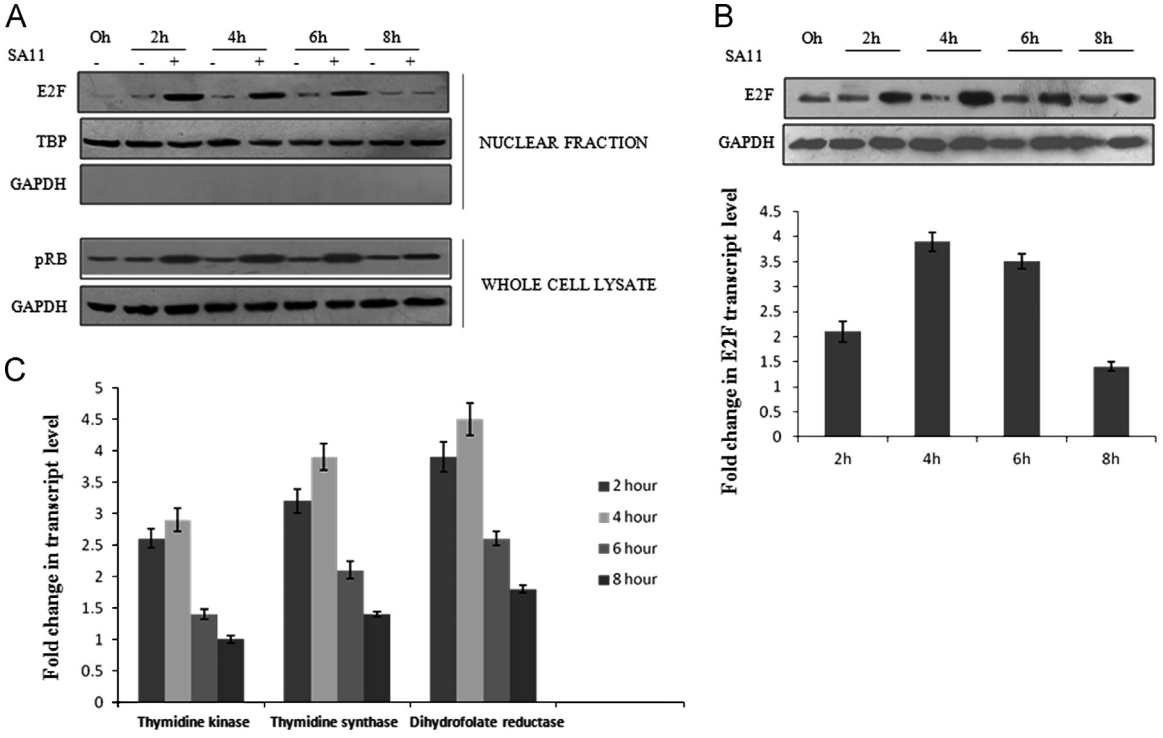

Fig. 2. RV infection induces E2F translocation by activating CDKs involved with G1 to S phase transition. (A) Whole cell lysates or nuclear fraction isolated by differential centrifugation of MA104 cells infected with SA11 were subjected to western blot analysis using pRb (lower panel) or E2F specific antibody (upper panel) respectively and compared with mock infected controls at corresponding time points. GAPDH and TBP were used as loading control for cellular or nuclear protein respectively. Results are representative of three independent experiments. (B) Whole cell lysates or total RNA from MA104 cells infected with SA11 for indicated time points were subjected to either western blot analysis using E2F and GAPDH (loading control) specific antibody or quantitative RT-PCR with E2F specific primers using SYBR Green dye and compared with mock infected controls. Fold changes of transcripts were obtained by normalizing relative gene expression (with respect to mock infected corresponding controls) to GAPDH using the formula $2^{-\Delta\Delta CT}$ ($\Delta\Delta CT = \Delta C_{T\ Sample} - \Delta C_{T\ Untreated\ control}$). Results are representative (mean ± SD) of three independent experiments. (C) Total RNA from MA104 cells infected with SA11 for indicated time points were isolated using TRIZOL and subjected to real time PCR with thymidine kinase, thymidine synthase, dihydrofolate reductase specific primer using SYBR Green dye. Fold changes of mRNA level were obtained by normalizing relative gene expression (with respect to mock infected corresponding controls) to GAPDH using the formula $2^{-\Delta\Delta CT}$ ($\Delta\Delta CT = \Delta C_{T\ Sample} - \Delta C_{T\ Untreated\ control}$). Results are representative (mean ± SD) of three independent experiments.

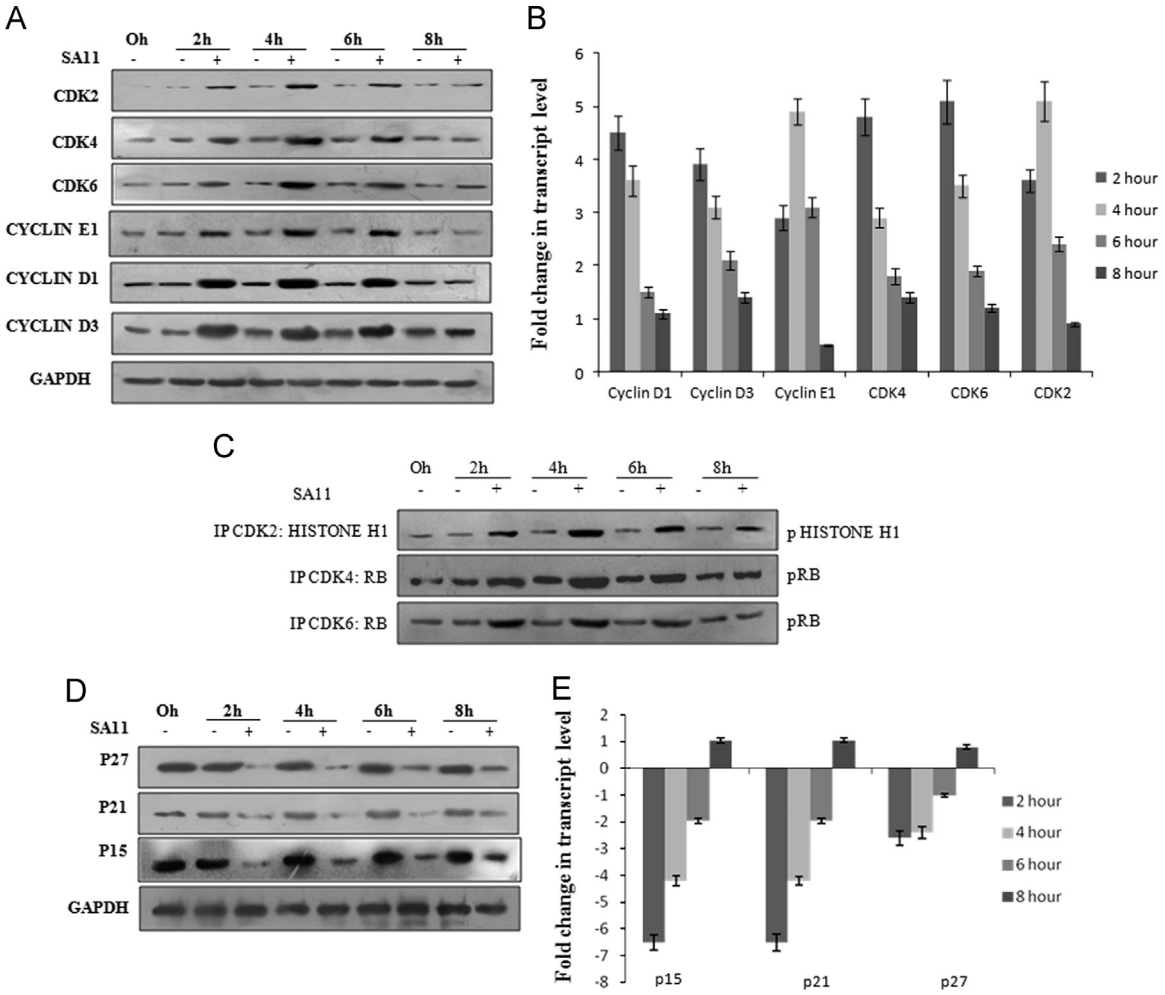

Fig. 3. RV infection up regulates expression of cyclin, CDK level but downregulates CDK inhibitors. (A, D) MA104 cells were infected with SA11 for indicated time points or kept mock infected followed by western blot analysis using Cyclin D1(A), Cyclin D3 (A), cyclin E1(A), CDK4 (A), CDK6 (A), CDK2 (A), p15 (D), p21 (D), p27 (D) specific antibodies. GAPDH was used as loading control. Results are representative of three independent experiments. (C) MA104 cells were either infected with SA11 or kept mock infected for indicated time points and subjected to immunoprecipitation with either CDK4 or CDK6 or CDK2 specific antibody. Immunoprecipitates were incubated with either Rb (for CDK4, CDK6) or Histone H1 (CDK2) followed by immunoblot analysis using pRb and pHistone H1 specific antibody. Results are representative of three independent experiments. (B, E) Total RNA from MA104 cells infected with SA11 for 2–8 hpi were isolated using TRIZOL (Invitrogen) and subjected to quantitative RT-PCR with cyclin D1 (B), cyclin D3 (B), cyclin E1 (B), CDK4 (B), CDK6 (B), CDK2 (B), p15 (E), p21 (E), p27 (E) specific primers using SYBR Green dye. Fold changes of transcripts were obtained by normalizing relative gene expression (with respect to mock infected corresponding controls) to GAPDH using the formula $2^{-\Delta\Delta CT}$ ($\Delta\Delta CT = \Delta C_{T\ \text{Sample}} - \Delta C_{T\ \text{Untreated control}}$). Results are representative (mean ± SD) of three independent experiments.

inhibitors of both INK4 and CIP/KIP family were significantly down regulated during early SA11 infection (2–6 hpi) (Fig. 3D and E).

RV infection drives G_1 to S phase transition in a Ca^{+2}/CaM dependent pathway

CAMKI is a CaM activated kinase which regulates G_1 to S phase progression of cell (Skelding et al., 2011). In a previous study from our group, CaM level was found to be modulated during RV infection (Weinberg, 1995). To know the activation level of CaMKI during RV infection, MA104 cells were infected with the RV SA11 strain (at a moi of 3) and incubated for 0–8 hpi. Cell extracts were immunoblotted with phospho CaMKI and CaM specific antibody. Results indicated increased phosphorylation (activation) of CaMKI along with upregulation of CaM expression during initial time points of infection (2–6 h), followed by decrease at 8 hpi (Fig. 4A). To delineate relation between CaMKI activation and cell cycle progression, MA104 cells were either infected with RV SA11 strain at 3 moi or kept mock infected in presence or absence of either calcium chelator BAPTA-AM which chelates Ca^{+2} ions (Chattopadhyay et al., 2013) and inhibits CaM activation or CaM inhibitor W7 which bind selectively to CaM and inhibit its downstream functions (Dhillon et al., 2003), for indicated time points followed by cell cycle analysis using flowcytometry (treatments were done post viral absorption). Quantitive analysis revealed that both BAPTA-AM and W7 inhibit cell cycle progression from G1 to S phase as found in only SA11 infected MA104 cells (Fig. 4B). Inhibition of CAMKI activation by using BAPTA-AM and W7 was proved by immunoblotting the cell extracts of SA11 infected or mock infected MA104 cells treated with BAPTA-AM and W7 with phospho CaMKI specific antibody (Fig. 4C). To define the mechanism behind Ca^{+2}/CaM activated CaMKI mediated cell cycle manipulation, we assessed the levels of Rb phosphorylation and E2F translocation to nucleus during SA11 infection in presence or absence of BAPTA-AM or W7 treatment. Both BAPTA-AM and W7 significantly minimized Rb phosphorylation and nuclear translocation of E2F compared to only virus infected cells (Fig. 5A). To know the effect of Ca^{+2} chelation and CaM inhibition during SA11 infection on cyclins, CDKs and CKIs associated with G1 to S phase transition, MA104 cells were either infected with

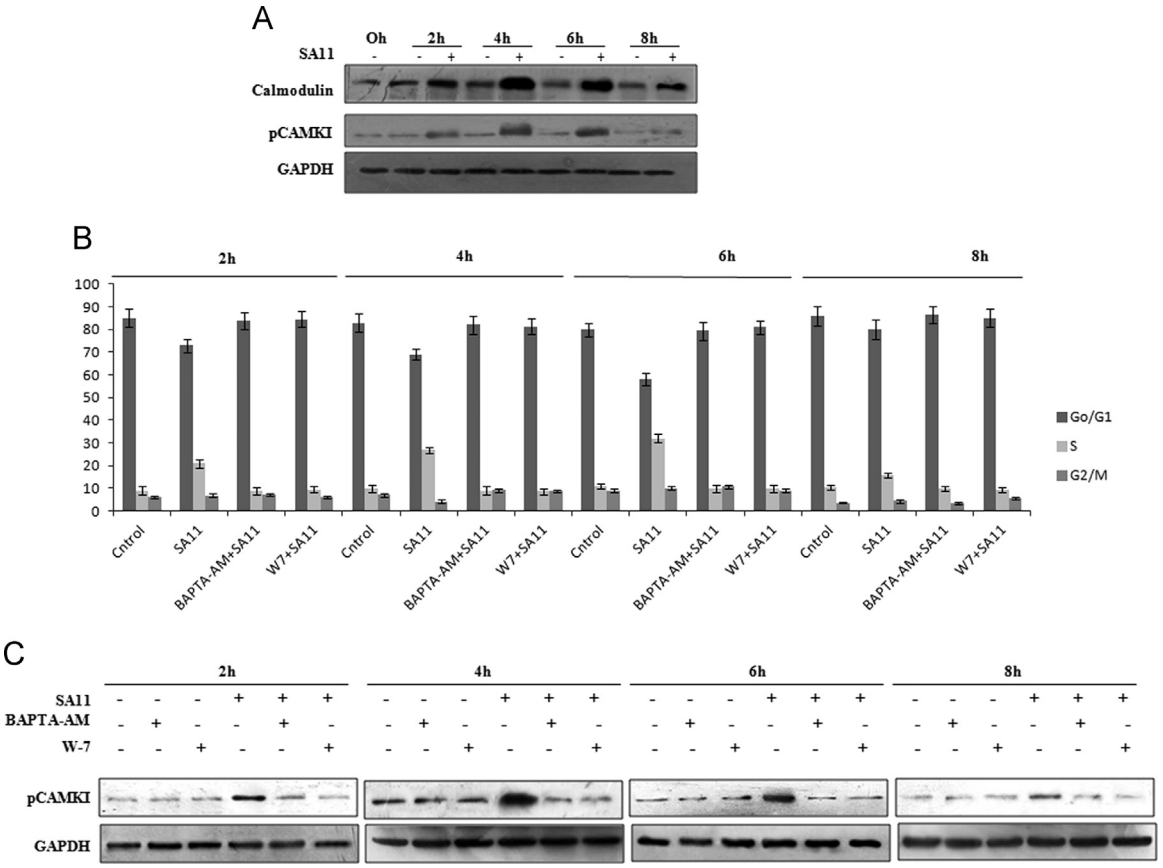

Fig. 4. RV infection activates CaMKI which leads to G1 to S phase progression. (A) Whole cell lysates isolated from MA104 cells infected with SA11 for indicated time points were subjected to western blot analysis using CaM, pCaMKI and GAPDH (loading control) specific antibody. Results are representative of three independent experiments. (B) MA104 cells were kept mock infected or infected with SA11 strain in presence or absence of W7 and BAPTA-AM for 2–8 h or kept mock infected followed by propidium iodide staining and cell cycle analysis using flow cytometer. Each bar represent % of cell present in specific phase of cell cycle. Results are representative (mean ± SD) of three independent experiments. (C) MA104 cells were kept mock infected or infected with SA11 strain in presence or absence of W7 and BAPTA-AM for 2–8 h or kept mock infected followed by western blot analysis using pCaMKI and GAPDH (loading control) specific antibody. Results are representative of three independent experiments.

SA11 or kept mock infected in presence or absence of either BAPTA-AM or W7 followed by immunoblotting with CDK2, CDK6, cyclin E1, cyclin D1, p27 and p21 specific antibodies. No significant change in expression level of cyclins and CDKs was observed in SA11 infected cells in presence of W7 or BAPTA-AM compared to mock infected control (Fig. 5B) confirming Ca^{+2}/CaM dependent CaMKI mediated upregulation of cyclin and CDK expression (Fig. 3A) during RV infection. But in case of CKIs, following RV infection, expression of p21 and p27 was downregulated both in presence (Fig. 5B) or absence (Fig. 3D) of BAPTA-AM and W7 suggesting that CKI regulation is Ca^{+2}/CaM independent.

Accumulation of cells in S phase during early infection is important for RV replication

Previous experiments showed RV infection drives cells from G_1 to S phase during early infection. To know the physiological relevance of this phenomenon during virus infection MA104 cells synchronized at G_0/G_1 phase (terfenadine treated) or at S phase (AZT treated) were infected with SA11 (moi 3) and expression of viral gene was assessed by either realtime PCR (Fig. 6A) or immunoblotting (Fig. 6B) with NSP3 specific primers or antibodies and compared with viral gene expression in infected unsynchronized cell. Result revealed in G_0/G_1 synchronized cells, viral gene expression was significantly low compared to unsynchronized cells but it was significantly higher in S phase synchronized cells (Fig. 6A and B). Furthermore, viral titers were measured by plaque assay in unsynchronized MA104 cells or cells synchronized at G_0/G_1 phase or at S phase following infection with SA11 strains at 1 moi. Compared to cells synchronized at G_0/G_1 phase significantly higher viral titers were observed in cells synchronized at S phase or unsynchronized cells (Fig. 6C). This is consistent with NSP3 expression pattern suggesting increased rotaviral replication during S phase.

Discussion

Entry into and progression through the cell cycle is considered as a key event in maintaining cellular homeostasis, anomalies in which can cause either cell death or can lead to uncontrolled cell division (Vermeulen et al., 2003). To ensure correct cell division in higher eukaryotes, cell cycle is intricately controlled by numerous complex mechanisms (Schafer, 1998), which in turn are manipulated by many viruses to favor their replication (Emmett et al., 2005). In our current study we found RV also influences cell cycle status of infected cells by propelling them from G_1 to S phase in a strain independent manner (Fig. 1A). Replication of RV is important for cell cycle manipulation as UV inactivated viruses could not drive G_1 to S phase transition (Fig. 1A) as well as level

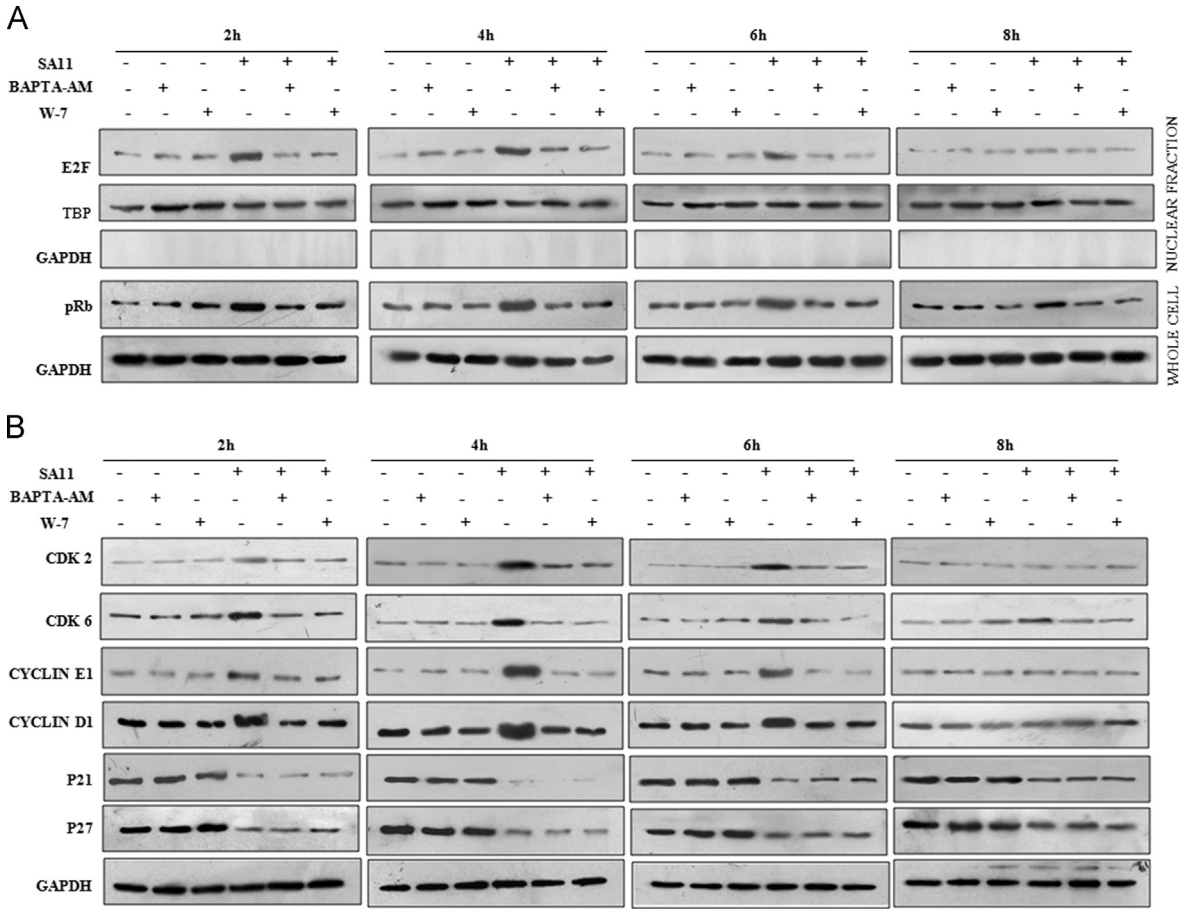

Fig. 5. Ca^{+2}/CaM pathway inhibition during RV infection prevents modulation of cell cycle regulatory proteins except CKIs. (A) MA104 cells were kept mock infected or infected with SA11 strain in presence or absence of W7 and BAPTA-AM for 2–8 h or kept mock treated and whole cell lysates or nuclear fraction isolated by differential centrifugation were subjected to western blot analysis using pRb (lower panel) or E2F specific antibody (upper panel) respectively and compared with mock infected controls of corresponding time points. GAPDH and TBP were used as loading control for whole cell lysate or nuclear lysate respectively. Results are representative of three independent experiments. (B) MA104 cells were kept mock infected or infected with SA11 strain in presence or absence of W7 and BAPTA-AM for 2–8 h or kept mock treated followed by western blot analysis using Cyclin D1, cyclin E1, CDK6, CDK2, p21, p27 specific antibodies. GAPDH was used as loading control. Results are representative of three independent experiments.

and activity manipulation of cell cycle machinery proteins (data not shown).

Phosphorylation status of Rb controls the transition from G_1 to S phase which was found to be hyper phosphorylated during initial stages of RV infection (Fig. 2A). This results in its inability to bind to and prevent nuclear translocation of E2F (Fig. 2A), since E2F in nucleus can activate transcription of several downstream genes like thymidine kinase, thymidine synthase and dihydrofolate reductase (Fig. 2C), which promote cell cycle progression and DNA replication, nuclear accumulation of E2F by RV during early infection facilitates G_1/S restriction point modulation in favor of RV replication. Up-regulation of *in vivo* thymidine kinase activity in mice infected with RV has also been previously reported (Collins et al., 1988).

Sequential regulation of Rb phosphorylation and E2F activation during interphase is controlled by specific cyclin-CDK complexes such as CDK4, CDK6, CDK2 and cyclins (Cyclin D1, D3 and E1) (Bloom and Cross, 2007). D type cyclins (Cyclin D1, Cyclin D3) preferably binds and activates CDK4 and CDK6 to hyper phosphorylate Rb and free the E2F protein to induce the expression of cyclin E1 and CDK2 which after forming the holoenzyme retains the hyper phosphorylated state of the Rb molecule (Malumbres and Barbacid, 2009). Concurrent to Rb phosphorylation pattern, all the CDKs involved in G_1 to S phase transition were activated during early hours of infection (Fig. 3C). Formation of active cyclin-CDK complex depends on expression level of Cyclins and CDKs (Malumbres and Barbacid, 2009), manipulation of which might be one of the mechanisms employed by viruses to activate CDK complex. As speculated up-regulation of all the cyclins and CDKs was observed at both transcript or protein levels during early infections (Fig. 3A and B). Other than the expression level of cyclins and CDKs which is essential for formation of the holo enzyme, CKIs play an important regulatory role to control CDK activation. There are two families of CKIs, CIP/KIP and INK4 family. The CIP/KIP family of proteins includes p21, p27 and p57, which are specific inhibitors of kinase activity of all type of CDKs; by contrast compounds of the INK4 family (p15, p16, p18, p19) prevent the association as well as function of only CDK4, CDK6 and D type cyclins (Besson et al., 2008). During RV infection, in addition to up-regulation of cyclins and CDKs, members of CKIs were significantly down-regulated at both transcript and protein levels, which may have additive effect on CDK activation (Fig. 3D and E). The level of change in transcript and protein levels of cyclins, CDKs or CKIs did not correlate exactly at all time points (Fig. 3A, B, D, and E) which could be due to inhibition of translation of cellular proteins by different mechanisms (like inhibition of nucleocytoplasmic RNA transport) (Rubio et al., 2013; Padilla-Noriega et al., 2002).

During time course study, progression of cells from G_1 to S phase during early RV infection but no further progression to M phase was observed. Blockage in S to M phase transition is employed by different viruses (Luo et al., 2013a,b) to recruit

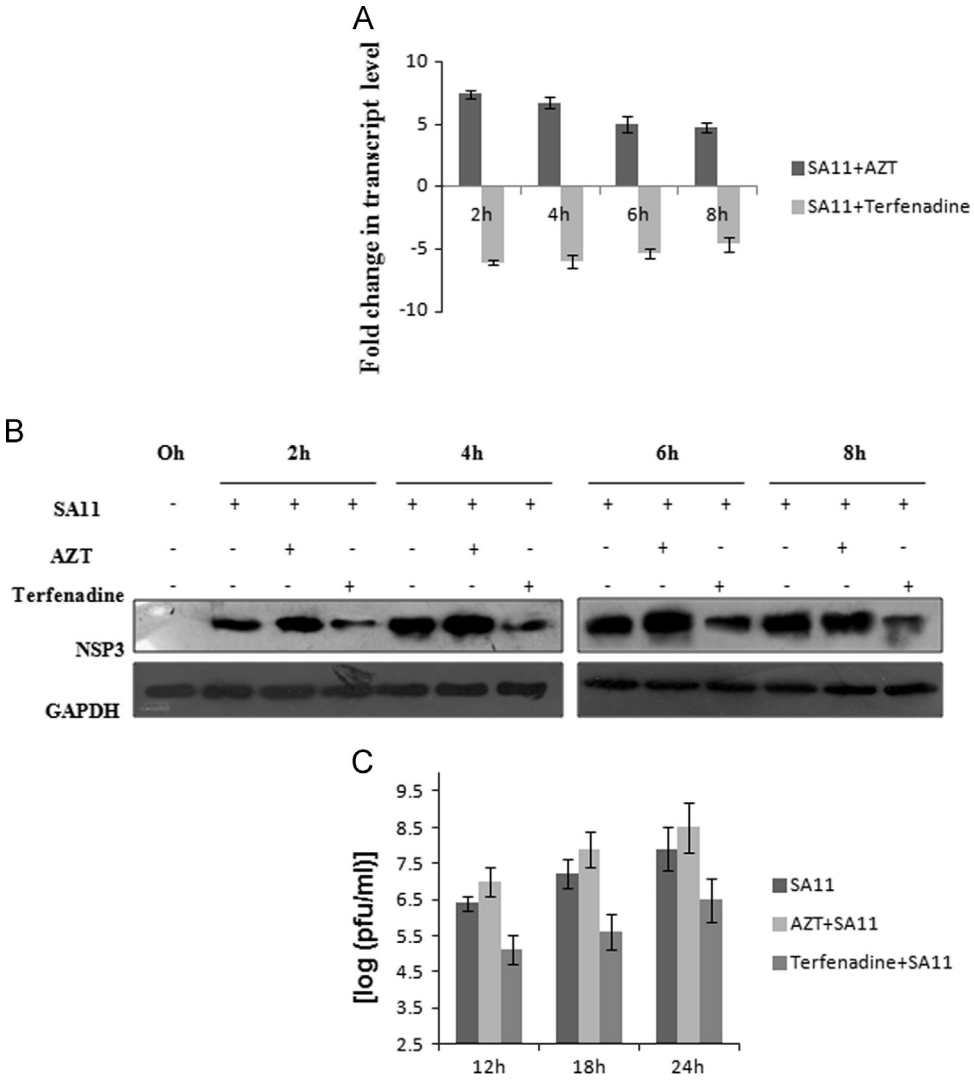

Fig. 6. Synchronization of cells at S phase assist RV replication while synchronization of cells at G0/G1 phase hampers it. (A) MA104 cells either synchronized in S (treated with AZT) phase or in G_0/G_1 phase (treated with terfenadine) or left unsynchronised were infected with SA11 for 2–8 hpi and total RNA was isolated and subjected to quantitative RT-PCR for viral gene expression and compared with SA11 infected unsynchronized cells. Fold changes of transcripts were obtained by normalizing relative gene expression (with respect to SA11 infected untreated cells) to GAPDH using the formula $2^{-\Delta\Delta CT}$ ($\Delta\Delta CT = \Delta C_{T\ \text{Sample}} - \Delta C_{T\ \text{Untreated control}}$). Results are representative (mean ± SD) of three independent experiments. (B) MA104 cells either synchronized in S (treated with AZT) phase or in G0/G1 phase (treated with terfenadine) or left unsynchronized were infected with SA11 for 28 hpi. Total lysates were subjected to westernblot analysis for viral gene expression (NSP3). (C) MA104 cells either synchronized either in S (treated with AZT) phase or in G0/G1 phase (treated with terfenadine) or left unsynchronized were infected for 12 hpi, 18 hpi, 24 hpi followed by Plaque assay. Viral titers were measured as plaque forming units [log (pfu/ml)]. Results are representative (mean ± SD) of three independent experiments.

cellular replication factors for viral replication. In case of rotavirus this could be due to stabilization of microtubules (Eichwald et al., 2012). In RV infection after accumulation of cells in S phase till 6 hpi, no of cells in G_0/G_1 phase started to increase (6 hpi and onwards) keeping consistency with the level of cyclins, CDKs, which started to decrease and CKIs, which were upregulated during 8 hpi. After that (10–12 hpi) activation of apoptotic pathways during late infection as observed in early studies by upregulation of p53 (Bhowmick et al., 2013), a modulator of cell cycle (Agarwal et al., 1995) was observed in cell cycle analysis of SA11 infected MA104 cells with increase in sub G_0 (apoptotic) population of cells (Fig. 1A).

Modulation of Ca^{+2} signals at various stages of the cell cycle and its role in cell cycle progression has been reported (Berridge et al., 2000) and Ca^{+2} concentrations was found to be increased during RV infection (Brunet et al., 2000). Versatile and complex Ca^{+2} signaling activates different Ca^{+2} binding proteins which then further modulate distinct cellular responses (Machaca, 2010). CaM is one of the important downstream effectors of Ca^{+2} which gets activated after binding Ca^{+2} (Chin and Means, 2000) and its expression levels have been linked to cell cycle progression both experimentally and physiologically (Choi and Husain, 2006). CaM expression is significantly increased during the G1–S transition (Chafouleas et al., 1982; Chafouleas et al., 1984). Increased expression of CaM during early hours (2–6 hpi) of RV infection has been observed in differential proteomics study by our group (Weinberg, 1995). CaM has been shown to activate several family of proteins namely serine/threonine phosphatase, calcineurin, multifunctional Ca^{2+}/CaM-dependent protein kinases, adenyl cyclises, ion channels, phosphodiesterases, myosin light chain kinases and protein phosphatises (Chin and Means, 2000) of which Ca^{2+}/CaM-dependent protein kinases have been shown to modulate cell cycle (Skelding et al., 2011). CaMKI has been shown to induce G_1 to S phase transition (Skelding et al., 2011), concurrently activation of CaMKI (phospho CaMKI) was also observed during early RV infection (2–6 hpi) which correlated with increased CaM expression and accumulation of cells in S phase (Fig. 4A). Significance of Ca^{+2}/CaM signaling in modulation of cell cycle during RV infection was

confirmed when Ca^{+2} chelator (BAPTA-AM) and CaM inhibitor (W7) inhibited G1 to S phase transition (Fig. 4B). Rb phosphorylation and nuclear translocation of E2F was also inhibited in presence of BAPTA-AM or W7 (Fig. 5A). Similar to Rb phosphorylation, expression levels of cyclins, CDKs were not modulated in presence of BAPTA-AM or W7 during RV infection (Fig. 5B), however the CKIs namely p21 and p27 were down regulated both in presence (Fig. 5B) or absence (Fig. 3D) of BAPTA-AM or W7. Down regulation of P21 and p27 is probably regulated by p53 which has been shown to be downregulated during early hours of RV infection (Bhowmick et al., 2013). Overall results suggest role of Ca^{+2}/CaM signaling in RV induced G1 to S phase transition. Ca^{+2}/CaM signaling is also important for RV replication as in presence of BAPTA-AM or W7 reduced viral titers were observed (Chattopadhyay et al., 2013; Pérez et al., 1998).

To further study relevance of G_1 to S phase transitions, during RV infection, specific inhibitors which can synchronize cells in S phase (AZT) or G_0/G_1 phase (Terfenadine) were used. AZT inhibits DNA replication by inhibiting thymidine kinase and preventing deoxythymidine triphosphate formation as a result it synchronizes cells at S phase (Chandrasekaran et al., 1995) whereas terfenadine prevents Rb phosphorylation and induce the level of CKIs to prevent cell cycle progression and synchronizes cells at G_0/G_1 phase (Liu et al., 2003). In RV infected S phase synchronized cells, increased viral gene expression and viral titers were observed whereas cells blocked in G_0/G_1 phase had reduced viral gene expression and titers compared to unsynchronized cells infected with SA11 confirming that RV induces G_1 to S phase transition for enhanced viral replication.

Overall the study focused on mechanism by which RV modulates the host cell cycle machinery. The results suggests a novel mechanism i.e. Ca^{+2}/CaM activation, employed by RVes to drive cells to accumulate in S phase by manipulating expression and activity of cell cycle regulatory proteins involved in G1 to S transition similar to hepatitis B virus (Yang and Cho, 2013; Benn and Schneider, 1995). Increase of cells in S phase during initial stages of infection was found to be beneficial for viral life cycle, which may be due to either stabilization of MT network during S phase which is helpful for viroplasm translocation (Eichwald et al., 2012) or increase in host replication proteins such as topo-isomerase during S phase which may assist in rotaviral replication as reported in case of ebola virus infection (Takahashi et al., 2013). It is also possible that S phase accumulation provides an anti-apoptotic environment for proper completion of viral replication cycle.

Materials and methods section

Cells, viruses and virus infection

The rhesus monkey epithelial cell line MA104 cells were cultured in minimal essential medium (MEM) supplemented with 10% heat-inactivated fetal bovine serum (FBS) and 1X PSF (penicillin, streptomycin and fungizone) at 37 °C humifiied incubator with 5% CO_2. SA11, A513 and and OSU strains of RV were used in this study (gifted by Prof. N. Kobayashi, Japan). For infection, viruses were activated with 0.1% acetylated trypsin (10 g/ml) (Gibco, Life Technologies, Carlsbad, CA) at 37 °C for 45 min (min) and added to the cells at 3 multiplicity of infection (moi, Infectious virus particles per cell) for 60 min at 37 °C. Unbound virus was removed by media wash and infection was continued in fresh MEM supplemented with 0.01% acetylated trypsin and antibiotic. The time of virus removal was taken as 0 h post infection for all experiments. Extracted and purified viral preparations were titrated by plaque assay (Smith et al., 1979).

Antibody, recombinant proteins and chemicals

Antibodies against E2F, GAPDH, CaM, phospho CaM kinase I, CDK2, cyclin E1, TBP were from Santa Cruz Biotechnology (Santa Cruz, CA). Antibody against Phospho-Rb (Ser807/811), CDK4, CDK6, cyclin D1, cyclin D3, p27, p21, p15 were from Cell signaling Technologies (Danvers, MA, USA). Phospho Histone H1 antibody was from Millipore (Billerica, MA, USA). All antibodies were used at dilutions recommended by the manufacture. Mouse polyclonal antibody against NSP3 was raised against full length recombinant protein according to standard protocols at the department of Virology and Parasitology, Fujita Health University School of Medicine, Aichi, Japan and used in 1:3000 dilutions. Recombinant retinoblastoma and histone H1 proteins were purchased from Sigma Aldrich (St. Louis, MO, USA). BAPTA-AM, AZT, Terfenadine were purchased from Sigma Aldrich and W7 was purchased from Santa Cruz Biotechnology.

Cytotoxicity assay

To determine cytotoxicity of AZT, Terfenadine, BAPTA-AM, W-7 in MA104 cells, cell viability assays were performed in 96-well plates ($\approx 5 \times 104$ cells/well). Cells were treated with the drugs as mentioned in Supplementary Fig. 1 for 24 h followed by an MTT assay (Sigma-Aldrich). Briefly, 10 mL of MTT solution (5 mg/mL in PBS) was added and incubated at 378 °C for 4 h. The formazan was dissolved in 200 mL DMSO and the optical density (OD) of the solution was measured at 570 nm and 630 nm to obtain the sample signal (OD570–OD630). The cytotoxicity was measured as cell viability compared with DMSO treated cells.

Immunoblot analysis

Whole cell lysates [extracted by incubating in ice for 15 min with Totex buffer (20 mM Hepes at pH 7.9, 0.35 M NaCl, 20% glycerol, 1% NP-40, 1 mM $MgCl_2$, 0.5 mM EDTA, 0.1 mM EGTA, 50 mM NaF and 0.3 mM Na_3VO_4) containing mixture of protease and phosphatase inhibitors (Sigma, St. Louis, MO), cytoplasmic or nuclear extracts or immunoprecipitated products were prepared. Samples were incubated in protein sample buffer (final concentration: 50 mM Tris, pH 6.8, 1% SDS, 10% glycerol, 1% β-mercaptoethanol, and 0.01% bromphenol blue) for 30 min at either 4 °C or, alternatively, boiled for 5 min before SDS-PAGE at room temperature followed by immunoblotting with specific antibodies as described previously (Chawla-Sarkar et al., 2004). Primary antibodies were identified with HRP conjugated secondary antibody (Pierce, Rockford, IL) and chemiluminescent substrate (Millipore, Billerica, MA). Where necessary, to confirm protein loading blots were reprobed with GAPDH or TBP. The immunoblots shown are representative of three independent experiments.

Real time PCR

Total RNA was isolated using TRIzol (Invitrogen, Grand Island, USA) according to the manufacturer's instructions. cDNA was prepared from 1 to 2 μg of RNA using the Superscript II reverse transcriptase (Invitrogen) with random hexamer primers. Real-time PCR reactions (50 °C for 2 min, 95 °C for 10 min, followed by 40 cycles of 95 °C for 15 s and 60 °C for 30 s and 72 °C for 10 min) were performed in triplicate using SYBR Green (Applied Biosystems, Foster City, CA, USA) in Step one plus (Applied Biosystems, Life Technologies, Carlsbad, CA) with primers specific for thymidine kinase, thymidine synthase and dihydrofolate reductase, CDK4, CDK6, CDK2, cyclin D1, cyclin D3, p27, p21, p15, cyclin E1 [Primer sequences are available on request]. The relative gene expressions were normalized to GAPDH using the formula $2^{-\Delta\Delta CT}$

(ΔΔCT = ΔCTSample − ΔCT Untreated control), where CT is the threshold cycle.

Sub cellular fractionation

For preparation of cytosolic and nuclear fraction cells were washed in ice-cold phosphate buffered saline (PBS), pH 7.2, then in hypotonic extraction buffer (HEB: 50 mM PIPES pH 7.4,50 mM KCl, 5 mM EGTA, 2 mM $MgCl_2$, 1 mM dithiothreitol and 0.1 mM phenyl methyl sulphonyl fluoride (PMSF)) and centrifuged. The pellet was re suspended in HEB and lysed in a Dounce homogenizer. This cell lysate was centrifuged for 10 min at 1000*g* at 4 °C to pellet nuclei and the clarified supernatant (cytosolic fraction) was stored at −80 °C. Nuclear fractions were prepared by re suspending the pellet in ice cold buffer C (10 mM HEPES pH 7.9, 500 mM NaCl, 0.1 mM EDTA, 0.1 mM EGTA, 0.1% NP-40, 1 mM DTT, 1 mM PMSF, 8 mg/ml aprotinin, 2 mg/ml leupeptin (pH 7.4)), and kept for 30 min on ice with intermittent vortexing. Resuspended fraction was then spun at 14,000*g* for 30 min at 4 °C and the supernatant (nuclear fraction) was stored at −80 °C.

Cell cycle analysis

For cell cycle analysis nuclear DNA content was measured using propidium iodide (PI) staining. Briefly, adherent MA104 cells were collected by treatment with trypsin-EDTA and were then washed with ice cold PBS. The cells were fixed in 1 ml of cold 70% ethanol overnight at 4 °C and resuspended in staining buffer (50 μg/ml PI [Sigma], 20 μg/ml RNase in PBS) for 20 min at 37 °C. PI-stained cells were then analyzed using FACS (FACSAria; BD), and at least 20,000 cells were counted for each sample. Data analysis was performed by using ModFit LT, version 2.0 (Verity Software House).

Synchronization of cells

In this study cells were either synchronized at S phase or G_0/G_1 phase as described previously with some modifications (Chandrasekaran et al., 1995; Liu et al., 2003). For S phase synchronization MA104 cells (50–60% confluent) were treated with 3'-azido-3'-deoxythymidine (AZT) (200 μM) in complete media (MEM, 10%FBS) for 24 h. For G_0/G_1 phase synchronization MA104 cells (80–90% confluent) were serum starved (MEM, 0.05% FBS) for 24 h followed by incubation with 5 μM terfenadine in complete media (MEM, 10%FBS) for 8 h. After that the cells were washed with PBS and subjected to infection in absence of drug as described previously.

In vitro kinase assay

To test kinase activity of CDK4, CDK6, CDK2 in mock and SA11 infected MA104 cells at increasing time points, cells were lysed in 50 mM Tris (pH 8.0), 0.5% NP-40, 2 mM EDTA, 137 mM NaCl, 10% glycerol, 2 mM sodium orthovanadate, 100 m M leupeptin, and 1 mM PMSF by incubating in ice for 30 min. Cell debris was removed by centrifugation and the supernatants were precleared with protein A-coupled agarose beads (Invitrogen) for 2 h. Then lysates (500 μg of protein each) were incubated at 4 °C with 1 μg of either anti-CDK2, or CDK4 or CDK6 specific antibody (Santa Cruz Biotechnology) in 0.5 μl of immunoprecipitation buffer (50 mM Tris, pH 8.0; 0.5% NP-40, 2 mM EDTA, 137 mM NaCl, 10% glycerol), collected on 25 μl of Protein A agarose beads, and washed twice with immunoprecipitation buffer and two times with kinase buffer (50 mM Tris, pH 7.4; 10 mM $MgCl_2$, 1 mM dithiothreitol). Kinase reactions were done in 25 μl of kinase buffer with 10 μg of substrate (histone H1 protein for CDK2 and retinoblastoma for CDK4, CDK6), 100 mM ATP. Reaction mixtures were incubated for 30 min at 37 °C and analyzed by immunoblotting with pRb and pHistone H1 specific antibodies after separation by SDS-PAGE.

Statistical analysis

Data are expressed as mean ± the standard deviations of at least three independent experiments ($n \geq 3$). In all tests, $P = 0.05$ was considered statistically significant.

Acknowledgments

This study was supported by the Indian Council of Medical Research (ICMR), New Delhi, and the Program for Funding Research Centers for Emerging and Reemerging Infectious Diseases (Okayama University–National Institute of Cholera and Enteric Diseases, India) from the Ministry of Education, Culture, Sports, Science, and Technology, Japan.

RB was supported by senior Research Fellowships from the Council of Scientific and Industrial Research (CSIR), India. GB was supported by BD Bioscience. SC was supported by junior Research Fellowships from the University Grants Commission (UGC), India and senior Research Fellowships from Indian Council of Medical Research (ICMR, India).

Appendix A. Supporting information

Supplementary data associated with this article can be found in the online version at http://dx.doi.org/10.1016/j.virol.2014.03.001.

References

Agarwal, M.L., Agarwal, A., Taylor, W.R., Stark, G.R., 1995. p53 controls both the G2/M and the G1 cell cycle checkpoints and mediates reversible growth arrest in human fibroblasts. Proc. Natl. Acad. Sci. USA 92, 8493–8497.

Alenzi, F.Q., 2004. Links between apoptosis, proliferation and the cell cycle. Br. J. Biomed. Sci., 99–102.

Autret, A., Martin-Latil, S., Brisac, C., Mousson, L., Colbère-Garapin, F., Blondel, B., 2008. Early phosphatidylinositol 3-kinase/Akt pathway activation limits poliovirus-induced JNK-mediated cell death. J. Virol. 82, 3796–3802.

Bagchi, P., Dutta, D., Chattopadhyay, S., Mukherjee, A., Halder, U.C., Sarkar, S., Kobayashi, N., Komoto, S., Taniguchi, K., Chawla-Sarkar, M., 2010. Rotavirus nonstructural protein 1 suppresses virus-induced cellular apoptosis to facilitate viral growth by activating the cell survival pathways during early stages of infection. J. Virol. 84, 6834–6844.

Bartek, J., Lukas, J., 2001. Pathways governing G1/S transition and their response to DNA damage. FEBS Lett. 490, 117–122.

Benn, J., Schneider, R.J., 1995. Hepatitis B virus HBx protein deregulates cell cycle checkpoint controls. Proc. Natl. Acad. Sci. USA 92, 11215–11219.

Berridge, M.J., Lipp, P., Bootman, M.D., 2000. The versatility and universality of calcium signaling. Nat. Rev. Mol. Cell Biol. 1, 11–21.

Besson, A., Dowdy, S.F., Roberts, J.M., 2008. CDK inhibitors: cell cycle regulators and beyond. Dev. Cell 14, 159–169.

Bhowmick, R., Halder, U.C., Chattopadhyay, S., Nayak, M.K., Chawla-Sarkar, M., 2013. RV-encoded nonstructural protein 1 modulates cellular apoptotic machinery by targeting tumor suppressor protein p53. J. Virol., 6840–6850

Bhowmick, Rahul, Chandra Halder, Umesh, Chattopadhyay, Shiladitya, Chanda, Shampa, Nandi, Satabdi, Bagchi, Parikshit, Kant Nayak, Mukti, Chakrabarti, Oishee, Kobayashi, Nobumichi, Chawla-Sarkar, Mamta, 2012. Rotaviral enterotoxin nonstructural protein 4 targets mitochondria for activation of apoptosis during infection. J. Biol. Chem. 287, 35004–35020.

Bitko, V., Shulyayeva, O., Mazumder, B., Musiyenko, A., Ramaswamy, M., Look, D.C., Barik, S., 2007. Nonstructural proteins of respiratory syncytial virus suppress premature apoptosis by an NF-kappaB-dependent, interferon-independent mechanism and facilitate virus growth. J. Virol. 81, 1786–1795.

Bloom, J., Cross, F.R., 2007. Multiple levels of cyclin specificity in cell-cycle control. Nat. Rev. Mol. Cell Biol. 8, 149–160.

Bollati, M., Milani, M., Mastrangelo, E., Ricagno, S., Tedeschi, G., Nonnis, S., Decroly, E., Selisko, B., de Lamballerie, X., Coutard, B., Canard, B., Bolognesi, M., 2009. Recognition of RNA cap in the Wesselsbron virus NS5 methyltransferase domain: implications for RNA-capping mechanisms in Flavivirus. J. Mol. Biol. 385, 140–152.

Brunet, J.P., Cotte-Laffitte, J., Linxe, C., Quero, A.M., Géniteau-Legendre, M., Servin, A., 2000. Rotavirus infection induces an increase in intracellular calcium

concentration in human intestinal epithelial cells: role in microvillar actin alteration. J. Virol. 74, 2323–2332.
Chafouleas, J.G., Bolton, W.E., Hidaka, H., Boyd III, A.E., Means, A.R., 1982. Calmodulin and the cell cycle: involvement in regulation of cell-cycle progression. Cell 28, 41–50.
Chafouleas, J.G., Lagace, L., Bolton, W.E., Boyd III, A.E., Means, A.R., 1984. Changes in calmodulin and its mRNA accompany reentry of quiescent (G0) cells into the cell cycle. Cell 36, 73–81.
Chandrasekaran, B., Kute, T.E., Duch, D.S., 1995. Synchronization of cells in the S phase of the cell cycle by 3'-azido-3'-deoxythymidine: implications for cell cytotoxicity. Cancer Chemother. Pharmacol. 35, 489–495.
Chattopadhyay, S., Basak, T., Nayak, M.K., Bhardwaj, G., Mukherjee, A., et al., 2013. Identification of cellular calcium binding protein calmodulin as a regulator of rotavirus A infection during comparative proteomic study. PLoS ONE 8 (2), e56655.
Chawla-Sarkar, M., Bae, S.I., Reu, F.J., Jacobs, B.S., Lindner, D.J., Borden, E.C., 2004. Downregulation of Bcl-2, FLIP or IAPs (XIAP and survivin) by siRNAs sensitizes resistant melanoma cells to Apo2L/TRAIL-induced apoptosis. Cell Death Differ. 11, 915–923.
Chen, C.J., Makino, S., 2004. Murine coronavirus replication induces cell cycle arrest in G0/G1 phase. J. Virol. 78, 5658–5669.
Chin, D., Means, A.R., 2000. Calmodulin: a prototypical calcium sensor. Trends Cell Biol. 10, 322–328.
Choi, J., Husain, M., 2006. Calmodulin-mediated cell cycle regulation: new mechanisms for old observations. Cell Cycle 5, 2183–2186.
Collins, J., Starkey, W.G., Wallis, T.S., Clarke, G.J., Worton, K.J., Spencer, A.J., Haddon, S.J., Osborne, M.P., Candy, D.C., Stephen, J., 1988. Intestinal enzyme profiles in normal and RV-infected mice. J. Pediatr. Gastroenterol. Nutr. 7, 264–272.
DeCaprio, J.A., Ludlow, J.W., Figge, J., Shew, J.Y., Huang, C.M., Lee, W.H., Marsilio, E., Paucha, E., Livingston, D.M., 1988. SV40 large tumor antigen forms a specific complex with the product of the retinoblastoma susceptibility gene. Cell 54, 275–283.
Dhillon, N.K., Sharma, S., Khuller, G.K., 2003. Influence of W-7, a calmodulin antagonist on phospholipid biosynthesis in Candida albicans. Lett. Appl. Microbiol. 36, 382–386, http://dx.doi.org/10.1046/j.1472-765X.2003.01324.x.
Dove, B., Brooks, G., Bicknell, K., Wurm, T., Hiscox, J.A., 2006. Cell cycle perturbations induced by infection with the coronavirus infectious bronchitis virus and their effect on virus replication. J. Virol. 80, 4147–4156.
Eckner, R., Ewen, M.E., Newsome, D., Gerdes, M., DeCaprio, J.A., Lawrence, J.B., Livingston, D.M., 1994. Molecular cloning and functional analysis of the adenovirus E1A-associated 300-kD protein (p300) reveals a protein with properties of a transcriptional adaptor. Genes Dev. 8, 869–884.
Ehrhardt, C., Wolff, T., Pleschka, S., Planz, O., Beermann, W., Bode, J.G., Schmolke, M., Ludwig, S., 2007. Influenza A virus NS1 protein activates the PI3K/Akt pathway to mediate antiapoptotic signaling responses. J. Virol. 81, 3058–3067.
Eichwald, C., Arnoldi, F., Laimbacher, A.S., Schraner, E.M., Fraefel, C., et al., 2012. Rotavirus viroplasm fusion and perinuclear localization are dynamic processes requiring stabilized microtubules. PLoS ONE 7e47947.
Emmett, S.R., Dove, B., Mahoney, L., Wurm, T., Hiscox, J.A., 2005. The cell cycle and virus infection. Methods Mol. Biol. 296, 197–218.
Estes, M.K., Kapikian, A.Z., 2007. 5th Ed. In: Knipe, D.M., Howley, P.M., Griffin, D.E., Lamb, R.A., Martin, M.A., Roizman, B., Straus, S.E. (Eds.), Fields Virology, vol. 2. Lippincott Williams & Wilkins, Philadelphia, pp. 1917–1974.
Fan, Jianguo, Bertino, Joseph R., 1997. Functional roles of E2F in cell cycle regulation. Oncogene 14, 1191–1200.
Fanning, E., Knippers, R., 1992. Structure and function of simian virus 40 large tumor antigen. Annu. Rev. Biochem. 61, 55–85.
Flemington, E.K., 2001. Herpesvirus lytic replication and the cell cycle: arresting new developments. J. Virol. 75, 4475–4481.
Foy, E., Li, K., Wang, C., Sumpter Jr, R., Ikeda, M., Lemon, S.M., Gale Jr, M., 2003. Regulation of interferon regulatory factor-3 by the hepatitis C virus serine protease. Science 300, 1145–1148.
Giacinti, C., Giordano, A., 2006. RB and cell cycle progression. Oncogene 25, 5220–5227.
Goh, W.C., Rogel, M.E., Kinsey, C.M., Michael, S.F., Fultz, P.N., Nowak, M. A, Hahn, B.H., Emerman, M., 1998. HIV-1 Vpr increases viral expression by manipulation of the cell cycle: a mechanism for selection of Vpr in vivo. Nat. Med. 4, 65–71.
Harbor, J.W., Dean, D.C., 2000. The Rb/E2F pathway: expanding roles and emerging paradigms. Genes Dev. 14, 2393–2409.
He, J., Choe, S., Walker, R., Di Marzio, P., Morgan, D.O., Landau, N.R., 1995. Human immunodeficiency virus type 1 viral protein R (Vpr) arrests cells in the G2 phase of the cell cycle by inhibiting p34cdc2 activity. J. Virol. 69, 6705–6711.
He, Y., Xu, K., Keiner, B., Zhou, J., Czudai, V, Li, T., Chen, Z., Liu, J., Klenk, H.D., Shu, Y.L., Sun, B., 2010. Influenza A virus replication induces cell cycle arrest in G0/G1 phase. J. Virol. 84, 12832–12840.
Holloway, G., Truong, T.T., Coulson, B.S., 2009. Rotavirus antagonizes cellular antiviral responses by inhibiting the nuclear accumulation of STAT1, STAT2, and NF-kappaB. J. Virol. 83, 4942–4951.
Howe, J.A., Mymryk, J.S., Egan, C., Branton, P.E., Bayley, S.T., 1990. Retinoblastoma growth suppressor and a 300-kDa protein appear to regulate cellular DNA synthesis. Proc. Natl. Acad. Sci. USA 87, 5883–5887.
Kahl, C.R., Means, A.R., 2003. Regulation of cell cycle progression by calcium/Calmodulin dependent pathways. Endocr. Rev. 24, 719–736.
Li, D., Gu, A.Z., He, M., Shi, H.C., Yang, W., 2009. UV inactivation and resistance of rotavirus evaluated by integrated cell culture and real-time RT-PCR assay. Water Res. 43, 3261–3269.
Liu, J.D., Wang, Y.J., Chen, C.H., Yu, C.F., Chen, L.C., Lin, J.K., Liang, Y.C., Lin, S.Y., Ho, Y.S., 2003. Molecular mechanisms of G0/G1 cell-cycle arrest and apoptosis induced by terfenadine in human cancer cells. Mol. Carcinog. 37, 39–50.
Luo, Y., Kleiboeker, S., Deng, X., Qiu, J., 2013a. Human parvovirus b19 infection causes cell cycle arrest of human erythroid progenitors at late s phase that favors viral DNA replication. J. Virol. 87, 12766–12775.
Luo, Y., Deng, X., Cheng, F., Li, Y., Qiu, J., 2013b. SMC1-mediated intra-S-phase arrest facilitates bocavirus DNA replication. J. Virol. 87, 4017–4032.
Machaca, K., 2010. $Ca^{(2+)}$ signaling, genes and the cell cycle. Cell Calcium 48, 243–250.
Malumbres, M., Barbacid, M., 2009. Cell cycle, CDKs and cancer: a changing paradigm. Nat. Rev. Cancer 9, 153–166.
Padilla-Noriega, Luis, Octavio Paniagua, 1, Guzmán-León, Simón, 2002. Rotavirus protein NSP3 shuts off host cell protein synthesis. Virology 298, 1–7.
Pérez, J.F., Chemello, M.E., Liprandi, F, Ruiz, M.C., Michelangeli, F., 1998. Oncosis in MA104 cells is induced by rotavirus infection through an increase in intracellular Ca^{2+} concentration. Virology 252, 17–27.
Rossen, J.W., Bouma, J., Raatgeep, R.H., Büller, H.A., Einerhand, A.W., 2004. Inhibition of cyclooxygenase activity reduces rotavirus infection at a postbinding step. J. Virol. 78, 9721–9730.
Roulston, A., Marcellus, R.C., Branton, P.E., 1999. Viruses and apoptosis. Annu. Rev. Microbiol., 577–628.
Rubio, R.M., Mora, S.I., Romero, P., Arias, C.F., López, S., 2013. Rotavirus prevents the expression of host responses by blocking the nucleocytoplasmic transport of polyadenylated mRNAs. J. Virol. 87, 6336–6345.
Schafer, K.A., 1998. The cell cycle: a review. Vet. Pathol. 35, 461–478.
Schang, L.M., 2003. The cell cycle, cyclin-dependent kinases, and viral infections: new horizons and unexpected connections. Prog. Cell Cycle Res. 5, 103–124.
Skelding, K.A., Rostas, J.A., Verrills, N.M., 2011. Controlling the cell cycle: the role of calcium/calmodulin-stimulated protein kinases I and II. Cell Cycle 10, 631–639.
Smith, E.M., Estes, M.K., Graham, D.Y., Gerba, C.P., 1979. A plaque assay for the simian rotavirus SAII. J. Gen. Virol. 43, 513–519.
Spann, K.M., Tran, K.C., Chi, B., Rabin, R.L., Collins, P.L., 2004. Suppression of the induction of alpha, beta, and lambda interferons by the NS1 and NS2 proteins of human respiratory syncytial virus in human epithelial cells and macrophages [corrected]. J. Virol. 78, 4363–4369.
Takahashi, K., Halfmann, P., Oyama, M., Kozuka-Hata, H., Noda, T., Kawaoka, Y., 2013. DNA topoisomerase 1 facilitates the transcription and replication of the Ebola virus genome. J. Virol. 87, 8862–8869.
Talon, J., Horvath, C.M., Polley, R., Basler, C.F., Muster, T., Palese, P., García-Sastre, A., 2000. Activation of interferon regulatory factor 3 is inhibited by the influenza A virus NS1 protein. J. Virol. 74, 7989–7996.
Vermeulen, K., Van Bockstaele, D.R., Berneman, Z.N., 2003. The cell cycle: a review of regulation, deregulation and therapeutic targets in cancer. Cell Proliferat. 36, 131–149.
Weinberg, R.A., 1995. The retinoblastoma protein and cell cycle control. Cell 81, 323–330.
Werness, B.A., Levine, A.J., Howley, P.M., 1990. Association of human papillomavirus types 16 and 18 E6 proteins with p53. Science 248, 76–79.
Yang, C.H., Cho, M., 2013. Hepatitis B virus X gene differentially modulates cell cycle progression and apoptotic protein expression in hepatocyte versus hepatoma cell lines. J. Viral Hepat. 20, 50–58.